

Dark matter distribution in dwarf spheroidal galaxies

Ewa L. Łokas

Nicolaus Copernicus Astronomical Center, Bartycka 18, 00–716 Warsaw, Poland

2 March 2019

ABSTRACT

We present predictions for the line-of-sight velocity dispersion profiles of dwarf spheroidal galaxies and compare them to observations in the case of the Fornax and Draco dwarfs. The predictions are made in the framework of standard dynamical theory of two-component (stars and dark matter) spherical systems with different velocity distributions. The stars are assumed to be distributed according to Sérsic laws with parameters fitted to observations. We discuss different dark matter density distributions, both cuspy and possessing flat density cores. For isotropic models the dark haloes with cores are found to fit the data better than those with cusps. Anisotropic models are studied by fitting two parameters, dark mass and velocity anisotropy, to the data. We find that the steeper the cusp of the profile, the more tangential is the velocity distribution required to fit the data, in agreement with the well-known degeneracy of density profile versus velocity anisotropy. However, only the profiles with cores yield good fits with anisotropy parameter close to the most natural, isotropic value. The results support the evidence based on studies of rotation curves of spiral galaxies which also favours density profiles with cores over those with cusps. We also show that with present quality of the data the alternative explanation of velocity dispersions in terms of Modified Newtonian Dynamics cannot yet be ruled out.

Key words: methods: analytical – galaxies: dwarf – galaxies: fundamental parameters – galaxies: kinematics and dynamics – cosmology: dark matter

1 INTRODUCTION

Dark matter is now generally believed to be the dominating component of the matter content of the Universe which has played an important role in the formation of structure. Significant effort has gone into establishing its properties and mechanisms of evolution. The theoretical results which got most attention in the recent years concerned the shape of density profiles of dark matter haloes. Those were mainly obtained by the means of *N*-body simulations with the most popular being the so-called universal profile advocated by Navarro, Frenk and White (1997, hereafter NFW). NFW found (and others confirmed) that in a large range of masses the density profiles of cold dark matter haloes forming in various cosmologies can be fitted with a simple formula with only one fitting parameter. This density profile steepens from r^{-1} near the centre of the halo to r^{-3} at large distances. More recent simulations with higher resolution produce even steeper density profiles, with inner slopes $r^{-3/2}$ (Fukushige & Makino 1997; Moore et al. 1998; see also Jing & Suto 2000).

Analytical calculations also predict density profiles with steep inner cusps. The NFW profile is claimed to be reproduced in studies taking into account the merging mechanism (Lacey & Cole 1993) in the halo formation scenario

(NFW, Avila-Reese, Firmani & Hernandez 1998). On the other hand, using an extension of the spherical infall model Łokas (2000) and Łokas & Hoffman (2000) have shown that if only radial motions are allowed the inner profiles have to be steeper than r^{-2} (in agreement with considerations based on distribution functions, see Richstone & Tremaine 1984). Although addition of angular momentum is known to make profiles shallower (White & Zaritsky 1992; Hiotelis 2001), its origin is not yet clear enough to make exact predictions.

The expected steep inner profiles are now being tested by comparison with observations of density profiles of galaxies and galaxy clusters. Recent studies of clusters (e.g. van der Marel et al. 2000) claim good agreement between cluster observations and the NFW mass density profile. In the case of galaxies, however, the situation is more troubling. Flores & Primack (1994) were the first to indicate that the NFW profile is incompatible with the rotation curves of spiral galaxies. More and more evidence is being presented now, which shows that spiral galaxies possess a dark matter core rather than a cusp in the inner parts (Burkert 1995; Salucci & Burkert 2000; Borriello & Salucci 2001). The evidence is especially convincing in the case of LSB galaxies which are supposed to be dominated by dark matter (de Blok et al. 2001; de Blok, McGaugh & Rubin 2001). Some mechanisms to explain the formation of such core have also been pro-

posed (Hannestad 1999; Kaplinghat, Knox & Turner 2000; El-Zant, Shlosman & Hoffman 2001; Ravindranath, Ho & Filippenko 2001).

Dwarf spheroidal (dSph) galaxies provide a unique testing tool for the presence and distribution of dark matter because due to their large velocity dispersions they are believed to be dominated by this component (for a review see Mateo 1997). Measurements of central velocity dispersion allowed many authors to estimate mass-to-light ratios in dwarfs and find it to be much larger than stellar values (see Mateo 1998 and references therein). These calculations were made with the simplifying assumption of isotropic velocity distribution. With the measured velocity dispersion profiles becoming available now, this assumption can in fact be relaxed and much more information can be extracted from the data. However, as in all pressure supported systems, when trying to model the velocity dispersion dependence on distance we are faced with the well-known degeneracy of density profile versus velocity anisotropy (Binney & Tremaine 1987).

The purpose of this work is to explore models for velocity dispersion profiles based on different dark matter density distributions and different assumptions concerning velocity anisotropy. We extend here the earlier work (Lokas 2001), which discussed only NFW profile, (see also Wilkinson et al. 2001; Kleyna et al. 2001a) by considering both cuspy profiles and those possessing flat cores, in order to decide which of them (and under what conditions) are favoured by observational data in the case of dSph galaxies.

The paper is organized as follows. In Section 2 we briefly describe the method of calculation of the line-of-sight velocity dispersion profile in models with different density profiles and velocity anisotropy. Section 3 describes the assumptions about the matter content of dSph galaxies. Results for the Fornax and Draco dwarfs for both isotropic and anisotropic velocity distribution are given in Section 4. The discussion follows in Section 5, where we also include comments on possible alternative explanation of velocity dispersions in terms of Modified Newtonian Dynamics (MOND).

2 VELOCITY DISPERSION PROFILE

The radial velocity dispersion $\sigma_r(r)$ of stars can be obtained by solving the Jeans equation (Binney & Tremaine 1987)

$$\frac{d}{dr}(\nu\sigma_r^2) + \frac{2\beta}{r}\nu\sigma_r^2 = \nu g, \quad (1)$$

where $\nu(r)$ is a 3D density of stars, $g(r)$ is the gravitational acceleration associated with the potential $\Phi(r)$, $g = -d\Phi/dr$, and $\beta = 1 - \sigma_\theta^2(r)/\sigma_r^2(r)$ is a measure of the anisotropy in the velocity distribution.

In the absence of direct measurements of velocity anisotropy in dSph galaxies we have to consider different values of β with the fiducial anisotropy model given by that of isotropic orbits: $\sigma_\theta(r) = \sigma_r(r)$ and $\beta = 0$. This case is not only the simplest to analyze but is also supported by the results of N -body simulations of dark matter haloes and observations of elliptical galaxies. For dark matter haloes Thomas et al. (1998) find that, in a variety of cosmological models, the ratio σ_θ/σ_r is not far from unity and decreases slowly with distance from the centre to reach $\simeq 0.8$ at the

virial radius. Observations of elliptical galaxies are also consistent with the orbits being isotropic near the centre and somewhat radially anisotropic farther away, although cases with tangential anisotropy are also observed (Gerhard et al. 2001).

Traditionally, β has been modelled in a way proposed by Osipkov (1979) and Merritt (1985) where $\beta_{OM} = r^2/(r^2 + r_a^2)$, with r_a being the anisotropy radius determining the transition from isotropic orbits inside to radial orbits outside. This model covers a wide range of possibilities from isotropy ($r_a \rightarrow \infty, \beta = 0$) to radial orbits ($r_a \rightarrow 0, \beta = 1$). Another possibility is that of tangential anisotropy with the fiducial case of circular orbits when $\beta \rightarrow -\infty$. For our purposes here it is most convenient to cover all possibilities from radial to isotropic and circular orbits with a simple model of $\beta = \text{const}$ and $-\infty < \beta \leq 1$.

The solution of the Jeans equation (1) with the boundary condition $\sigma_r \rightarrow 0$ at $r \rightarrow \infty$ for $\beta = \text{const}$ is

$$\nu\sigma_r^2(\beta = \text{const}) = -r^{-2\beta} \int_r^\infty r^{2\beta} \nu g \, dr. \quad (2)$$

From the observational point of view, an interesting, measurable quantity is the line-of-sight velocity dispersion obtained from the 3D velocity dispersion by integrating along the line of sight (Binney & Mamon 1982)

$$\sigma_{\text{los}}^2(R) = \frac{2}{I(R)} \int_R^\infty \left(1 - \beta \frac{R^2}{r^2}\right) \frac{\nu\sigma_r^2 r}{\sqrt{r^2 - R^2}} \, dr, \quad (3)$$

where $I(R)$ is the surface brightness.

Introducing result (2) into equation (3) and inverting the order of integration the calculations of σ_{los} can be reduced to one-dimensional numerical integration of a formula involving special functions for arbitrary $\beta = \text{const}$.

3 MATTER CONTENT

We will now discuss different mass distributions contributed by stars and dark matter to gravitational acceleration g in equation (1).

3.1 Stars

The distribution of stars is modelled in the same way as in Lokas (2001) i.e. by the Sérsic profile (Sérsic 1968, see also Ciotti 1991)

$$I(R) = I_0 \exp[-(R/R_s)^{1/m}], \quad (4)$$

where I_0 is the central surface brightness and R_s is the characteristic projected radius of the Sérsic profile. The Sérsic parameter m may vary in the range $1 \leq m \leq 10$ (Caon, Cappioli & D'Onofrio 1993) for different elliptical galaxies, however for dSph systems $m = 1$ is usually used, although in some cases other values of m are found to provide better fits (e.g. Caldwell 1999).

The 3D luminosity density $\nu(r)$ is obtained from $I(R)$ by deprojection

$$\nu(r) = -\frac{1}{\pi} \int_r^\infty \frac{dI}{dR} \frac{dR}{\sqrt{R^2 - r^2}}. \quad (5)$$

In the case of $m = 1$ we get $\nu(r, m = 1) = I_0 K_0(r/R_S)/(\pi R_S)$, where $K_0(x)$ is the modified Bessel function of the second kind. For other values of m in the range $1/2 \leq m \leq 10$ an excellent approximation for $\nu(r)$ is provided by (Lima Neto, Gerbal & Márquez 1999)

$$\begin{aligned} \nu(r) &= \nu_0 \left(\frac{r}{R_S} \right)^{-p} \exp \left[- \left(\frac{r}{R_S} \right)^{1/m} \right] \quad (6) \\ \nu_0 &= \frac{I_0 \Gamma(2m)}{2R_S \Gamma[(3-p)m]} \\ p &= 1.0 - 0.6097/m + 0.05463/m^2. \end{aligned}$$

The mass distribution of stars following from (6) is

$$M_*(r) = \Upsilon L_{\text{tot}} \frac{\gamma[(3-p)m, (r/R_S)^{1/m}]}{\Gamma[(3-p)m]}, \quad (7)$$

where $\Upsilon = \text{const}$ is the mass-to-light ratio for stars, L_{tot} is the total luminosity of the galaxy and $\gamma(\alpha, x) = \int_0^x e^{-t} t^{\alpha-1} dt$ is the incomplete gamma function.

3.2 Dark matter

We explore here different density distributions of dark matter which can be described by the following general formula

$$\rho(r) = \frac{\rho_{\text{char}}}{(r/r_s)^\alpha (1+r/r_s)^{3-\alpha}}, \quad (8)$$

where ρ_{char} is a constant characteristic density. As is immediately clear from equation (8), the inner slope of the profile is $r^{-\alpha}$ while the outer one is always r^{-3} . We choose the parameter α in the range $0 \leq \alpha \leq 3/2$, which covers a wide range of possible inner profiles. The cuspy profiles of $\alpha > 0$ are motivated by the results of N -body simulations. The profile with $\alpha = 1$ corresponds to the so-called universal profile proposed by NFW (see also Lokas & Mamon 2001) as a fit to the profiles of simulated haloes, while the profile with $\alpha = 3/2$ is identical to the one following from higher resolution simulations of Moore et al. (1998). The profile with $\alpha = 0$, possessing an inner core is favoured by observations of spiral galaxies (see the Introduction) and is very similar (but not identical) to the profile proposed by Burkert (1995).

The scale radius r_s introduced in equation (8) marks the distance from the centre of the object where the slope of the profile is the average of the inner and outer slope: $r^{-(3+\alpha)/2}$. Additional parameter which controls the shape of the profile is the concentration which we define here in a traditional way as

$$c = \frac{r_v}{r_s}, \quad (9)$$

where r_v is the virial radius, i.e. the distance from the centre of the halo within which the mean density is $v \approx 200$ times the present critical density, $\rho_{\text{crit},0}$.

We normalize the density profile (8) so that the mass within r_v is equal to the so-called virial mass

$$M_v = \frac{4}{3} \pi r_v^3 v \rho_{\text{crit},0}. \quad (10)$$

The characteristic density of equation (8) then becomes

$$\rho_{\text{char}} = \frac{(3-\alpha)v\rho_{\text{crit},0} c^\alpha}{3F(c)}, \quad (11)$$

where $F(c)$ is given by the hypergeometric function

$$F(x) = {}_2F_1(3-\alpha, 3-\alpha; 4-\alpha; -x). \quad (12)$$

The dark mass distribution following from (8), (10) and (11) is

$$M_{\text{D}}(s) = M_v s^{3-\alpha} \frac{F(cs)}{F(c)}, \quad (13)$$

where we introduced $s = r/r_v$.

The concentration of simulated dark matter haloes has been observed to depend on the virial mass. Using the N -body results for Λ CDM cosmology of Jing & Suto (2000) we find that this dependence can be approximated by the following formulae. In the case of $\alpha = 1$

$$c(\alpha = 1) = 10.23 \left(\frac{h M_v}{10^{12} M_\odot} \right)^{-0.088}, \quad (14)$$

while for $\alpha = 3/2$

$$c(\alpha = 3/2) = 4.877 \left(\frac{h M_v}{10^{12} M_\odot} \right)^{-0.131}, \quad (15)$$

where h is the Hubble constant in units of $100 \text{ km s}^{-1} \text{ Mpc}^{-1}$. In the following we will use $h = 0.7$.

Jing & Suto (2000) tested the relation $c(M_v)$ only for the masses of the order of normal galaxies and clusters so an extrapolation is needed in order to use them for dwarf galaxies. This was the approach used in the previous work (Lokas 2001). Here, however, similar relation would be needed for the $\alpha = 0$ profile and the information provided by observations is very scarce. Although relations e.g. between the inner mass and core radius have been found in the case of Burkert profile (Burkert 1995) and those can be translated into an $c(M_v)$ relation useful here, the estimates of this kind have been performed only for a small number of spiral galaxies and the errors of the fitted parameters are large (Borriello & Salucci 2001). We have therefore decided to assume different concentration parameters $c = \text{const}$ in the further analysis. Relations like (14)-(15) can however give an estimate of the order of magnitude of c in the case of cuspy profiles, i.e. for masses $10^5 M_\odot < M_v < 10^{14} M_\odot$ formula (14) gives approximately $7 < c(\alpha = 1) < 43$ while from (15) we get $3 < c(\alpha = 3/2) < 42$.

4 RESULTS FOR THE FORNAX AND DRACO DWARFS

4.1 Isotropic orbits

The observational parameters of the Fornax and Draco dwarfs needed in the following computation were taken from Irwin & Hatzidimitriou (1995) and are summarized in Table 1. The table gives the fitted Sérsic radius R_S assuming the $m = 1$ Sérsic distribution of equation (4), the distance modulus $m - M$, the brightness of the galaxies in V-band, M_V , and the total luminosity in V-band, $L_{\text{tot},V}$, together with its error. We adopt the mass-to-light ratio for stars in this band to be $\Upsilon_V \approx 1 M_\odot/L_\odot$ (Mateo et al. 1991).

In the previous work (Lokas 2001) it was shown that the density of stars alone cannot produce the observed velocity dispersion profiles in the case of Fornax and Draco. In the following we will explore the hypothesis that the velocity

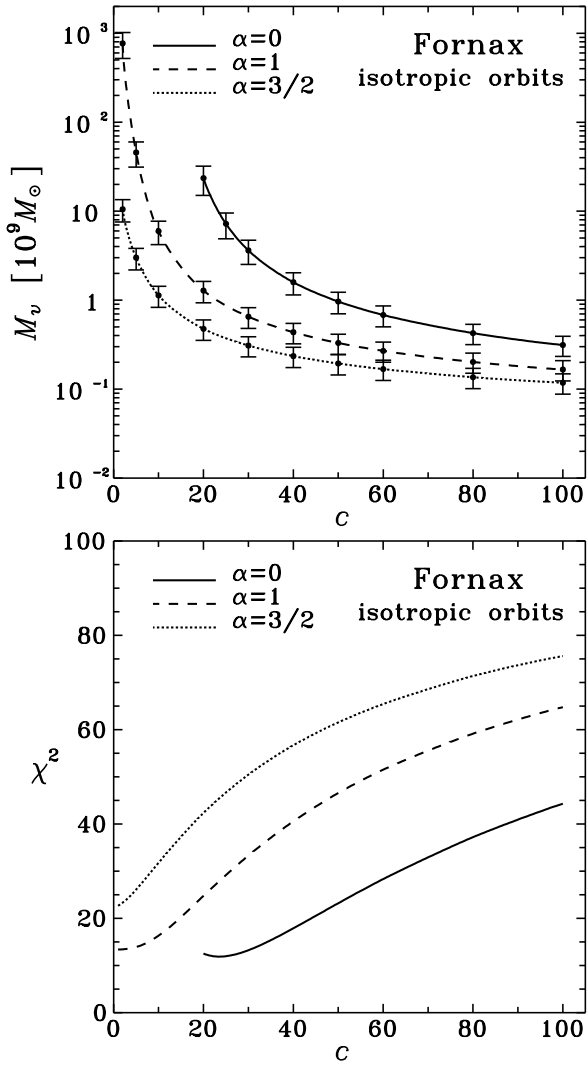


Figure 1. Upper panel: the best fitting masses of dark haloes as a function of assumed concentration parameter for profiles with different α in the case of isotropic orbits for the Fornax dwarf. Lower panel: the goodness of fit measure, χ^2 , for the fits in the upper panel.

Table 1. Observational parameters of the Fornax and Draco dwarfs from Irwin & Hatzidimitriou (1995).

parameter	Fornax	Draco
R_S (arcmin)	9.9	4.5
R_S (kpc)	0.35	0.094
$m - M$	20.4	19.3
distance (kpc)	120	72
M_V (mag)	-13.0	-8.3
$L_{\text{tot},V}(L_\odot)$	$(1.4 \pm 0.4) \times 10^7$	$(1.8 \pm 0.8) \times 10^5$

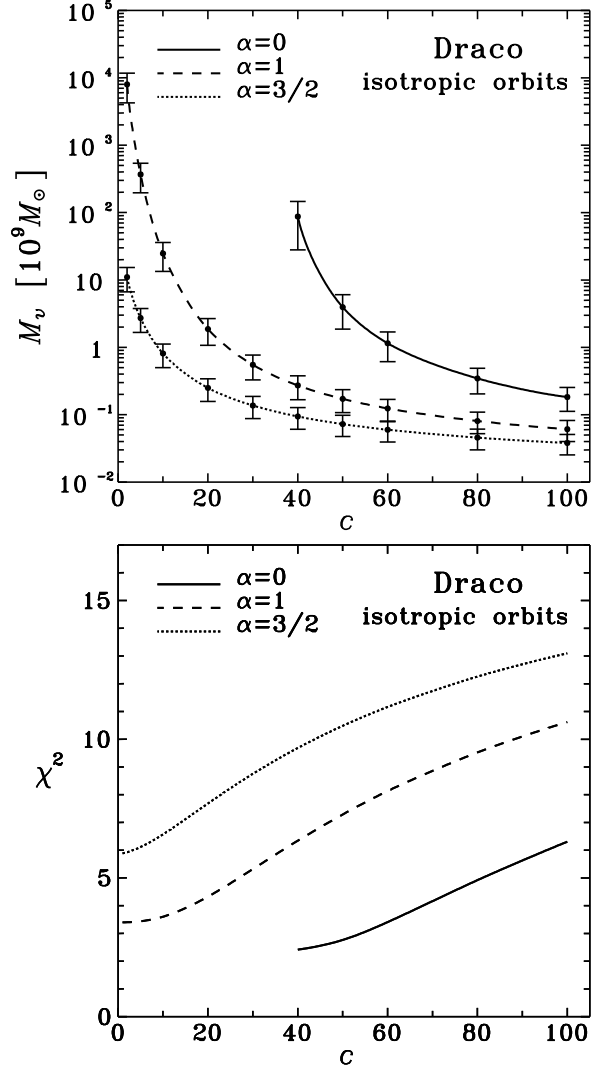


Figure 2. Same as Figure 1, but for Draco.

dispersions are generated by stars moving in the Newtonian gravitational acceleration generated by stars and dark matter.

We first assume that the velocity distribution of stars is isotropic, i.e. we consider models obtained from equations (2) and (3) in the case of $\beta = 0$. The 3D distribution of stars $\nu(r)$ is given by (6). The gravitational acceleration is $\mathbf{g} = -GM(r)/r^2$ with $M(r) = M_*(r) + M_D(r)$, where $M_*(r)$ and $M_D(r)$ are given by equations (7) and (13), respectively. Using such modelling of the velocity dispersion profile we perform a one-parameter fitting of the velocity dispersion data. In the case of Fornax we use the data of Mateo (1997) and in the case of Draco those of Armandroff, Pryor & Olszewski 1997 (based on the observations of Armandroff, Olszewski & Pryor 1995). In each case we assume the value of the concentration parameter c and fit by the least square method the dark virial mass M_v of the models with different dark matter profiles distinguished by the parameter α of equations (8) and (13).

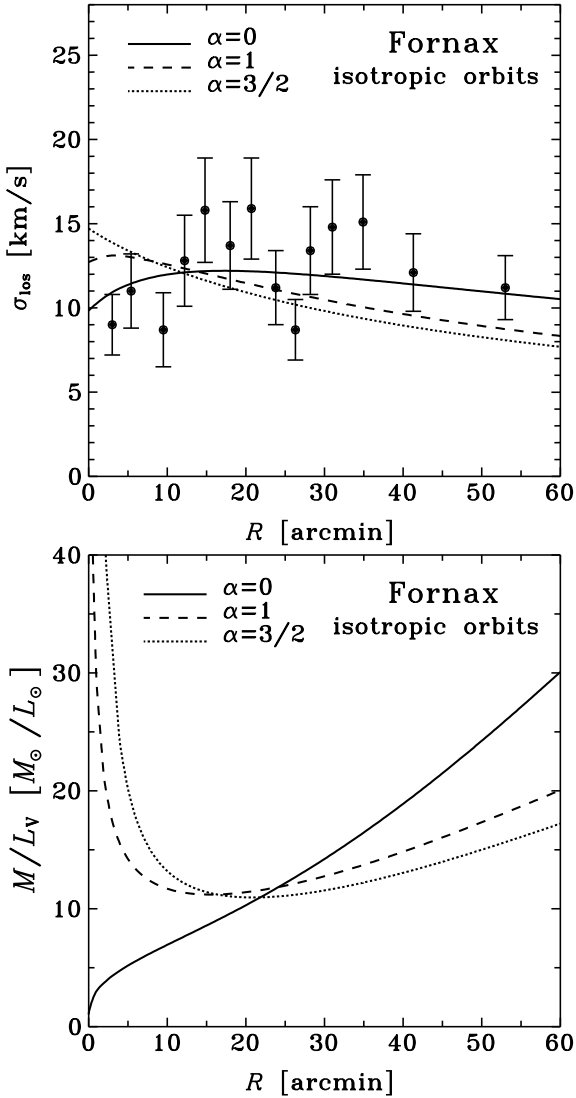


Figure 3. Upper panel: the best fitting velocity dispersion profiles obtained for $c = 30$ ($\alpha = 0$), $c = 20$ ($\alpha = 1$) and $c = 10$ ($\alpha = 3/2$) in the case of isotropic orbits for the Fornax dwarf. Lower panel: mass-to-light ratios for the fits in the upper panel.

The resulting best-fitting values of M_v as a function of assumed c are shown in the upper panels of Figures 1 and 2. The error bars indicate 1σ errors in M_v associated with the errors in the velocity dispersion measurements. The errors in mass in the whole range of concentrations shown in Figures 1 and 2 are of the order of 25–36% for Fornax and 34–70% for Draco. The lower panels of these Figures plot χ^2 , the measure of the goodness of fits presented in the upper panels. The results for $\alpha = 0$ do not reach to very low concentration because the least-square fitting converges more and more slowly there yielding incredibly high dark masses. One might think that a two-parameter (c, M_v) fitting would be a better choice here, but as the lower panels of Figures 1 and 2 show, this would give the lowest possible c in all cases. In the case of cuspy profiles resulting from N -body simulations low c of the order of unity is never obtained except for objects of the mass of cluster of galaxies. Clearly for both Fornax and

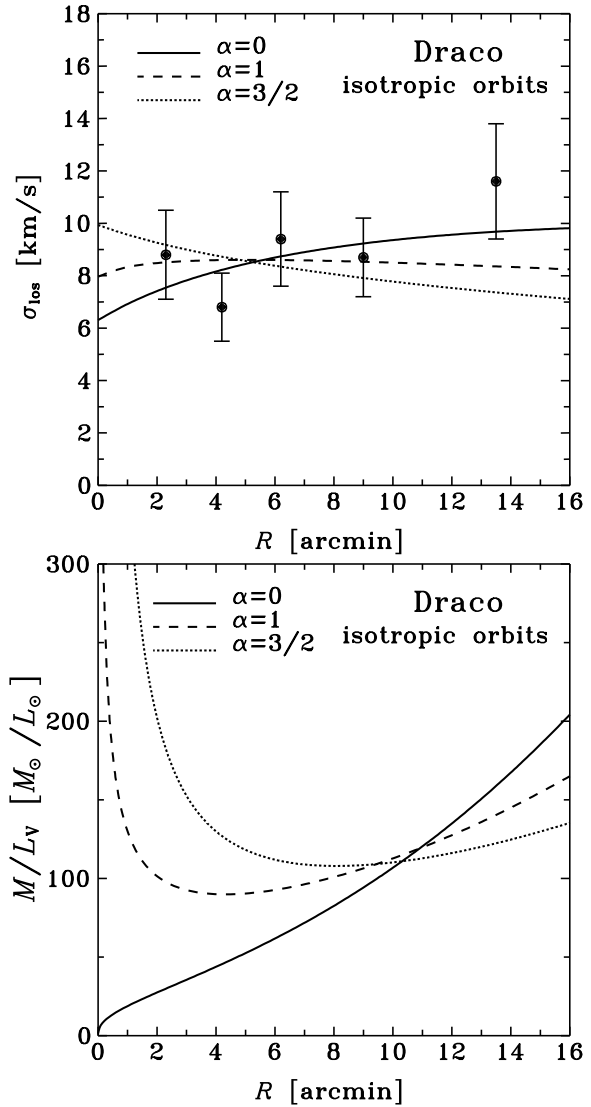


Figure 4. Same as Figure 3, but for Draco. The best fitting velocity dispersion profiles plotted were obtained for $c = 50$ ($\alpha = 0$), $c = 20$ ($\alpha = 1$) and $c = 10$ ($\alpha = 3/2$).

Draco the $\alpha = 0$ profile provides the best fit in terms of χ^2 . Although quite low χ^2 can be also obtained for $\alpha = 1$ profile, this happens only for unrealistic low concentrations and yielding incredibly high mass of a halo of the order of a normal galaxy.

The predictions for the line-of-sight velocity dispersion profiles of the best-fitting models with $\alpha = 0, 1$ and $3/2$ in the isotropic case are shown in the upper panels of Figures 3 and 4 for Fornax and Draco respectively together with the data. For clarity of the illustration we have chosen only one of the fits from Figures 1 and 2 for each type of profile. In the case of $\alpha = 0$ profile no a priori information on c is available so we have chosen the value giving the best fit and reasonably low best-fitting mass M_v at the same time, i.e. $c = 30$ in the case of Fornax and $c = 50$ in the case of Draco. For cuspy profiles the concentrations acceptable from the point of view of the N -body results i.e. in rough

Table 2. Examples of best-fitting parameters in the isotropic and anisotropic case with 1σ error bars. M_v is given in units of $10^9 M_\odot$.

case	α	parameter	Fornax	Draco
$\beta = 0$	0	M_v	3.6 ± 1.1	3.9 ± 2.1
	1	M_v	1.3 ± 0.4	1.9 ± 0.8
	3/2	M_v	1.1 ± 0.3	0.81 ± 0.31
$\beta \neq 0$	0	M_v	3.4 ± 0.6	4.3 ± 1.2
		β	-0.36 ± 0.31	-0.094 ± 0.50
	1	M_v	1.3 ± 0.2	2.4 ± 0.7
$\beta = 0$		β	-1.5 ± 0.8	-0.97 ± 1.2
	3/2	M_v	1.2 ± 0.2	1.2 ± 0.4
		β	-2.6 ± 1.5	-3.5 ± 5.1

agreement with formulae (14) and (15) were chosen. We have taken $c = 20$ for $\alpha = 1$ and $c = 10$ for $\alpha = 3/2$. The best-fitting virial masses obtained for these concentrations in the isotropic case together with 1σ error bars are given in the upper part of Table 2.

Lower panels of Figures 3 and 4 show the combined mass-to-light ratio in V-band for Fornax and Draco calculated from

$$M/L_V = \frac{M_D(r) + M_*(r)}{L_V(r)}, \quad (16)$$

where $M_D(r)$ and $M_*(r)$ are given by equations (13) and (7) respectively, and $L_V(r) = M_*(r)/\Upsilon_V$ is the luminosity distribution. Calculation of M/L_V were made for the same models as presented in the upper panels of the Figures.

The growth of M/L_V at large distances is due to the behaviour of $M_D(r)$ which diverges logarithmically for all considered α while the mass in stars is finite. However, while the cuspy profiles produce divergent M/L_V at the centre of the galaxy, the $\alpha = 0$ profile gives a more realistic, finite M/L_V increasing at all radii. All the mass-to-light estimates shown give a similar $M/L_V \approx 10M_\odot/L_\odot$ in the case of Fornax and $M/L_V \approx 100M_\odot/L_\odot$ in the case of Draco at a scale of the order of two Sérsic radii and are consistent with the values of the central mass-to-light ratios estimated by Mateo et al. (1991) and Armandroff et al. (1997).

4.2 Anisotropic orbits

Comparing the predictions shown in upper panels of Figures 3 and 4 with the data we find that the cuspy profiles have to be aided by a certain amount of tangential anisotropy in order to better reproduce the shape of the observed velocity dispersion profiles. Trying more radial anisotropy than in the case of isotropic orbits by using positive values of β makes the curves decrease even more steeply with distance, contrary to the trend observed in the data. In the case of the profile with $\alpha = 0$ it is not clear whether more radial or more tangential anisotropy would provide a better fit. Therefore in what follows we perform a two-parameter fitting of the velocity dispersion profiles with velocity anisotropy $\beta = \text{const}$ as a second free parameter in addition to the dark mass, M_v .

The results of such least-square fitting procedure of the Fornax and Draco data are shown in Figures 5 and 6. The

Figures are analogous to Figures 1 and 2 for the isotropic case except for the added uppermost panels showing the best-fitting β parameters with their 1σ error bars. The estimated dark virial masses in the middle panels are now roughly the same for Fornax and somewhat higher for Draco than for isotropic orbits while their errors are decreased to 18% for Fornax and 28-30% for Draco for the whole range of concentrations. The quality of fits (bottom panels) is now significantly better for cuspy profiles and also somewhat improved for the profiles with $\alpha = 0$. However, the profiles with cores produce best-fitting β closest to zero.

Figures 7 and 8 are the anisotropic analogues of Figures 3 and 4. As in the isotropic case for $\alpha = 0$ profile we have chosen $c = 30$ in the case of Fornax and $c = 50$ in the case of Draco, while for cuspy profiles we have taken $c = 20$ for $\alpha = 1$ and $c = 10$ for $\alpha = 3/2$. These values of concentrations happen to be those where χ^2 reaches minimum for different profiles in the case of Fornax (see the lowest panel of Figure 5). The corresponding best-fitting values of M_v and β are given in the lower part of Table 2.

It is clear from the upper panels of Figures 7 and 8 that when arbitrary anisotropy parameters are allowed acceptable fits can be obtained with all profiles. However, cuspy profiles require significantly more tangential anisotropy, i.e. lower β than the profile possessing a core. The mass-to-light ratios shown in the lower panels of Figures 7 and 8 do not change significantly with respect to the isotropic case and the very different behaviour for cuspy profiles versus profile with a core is preserved.

5 DISCUSSION

5.1 Conclusions

We presented predictions for the line-of-sight velocity dispersion profiles of dwarf spheroidal galaxies and compared them to observations in the case of the Fornax and Draco dwarfs. We discussed different dark matter distributions, both cuspy and possessing flat density cores. For isotropic models the dark haloes with cores are found to generally fit the data better than those with cusps. Although acceptable fits can also be found for cuspy profiles in this case, it is possible only for very low concentrations characteristic of much larger masses of haloes obtained in N -body simulations and incredibly high corresponding dark masses of the order of a normal galaxy.

Anisotropic models were studied by fitting two parameters, dark mass and velocity anisotropy, to the data. We find that the steeper the cusp of the profile, the more tangential is the velocity distribution required to fit the data, in agreement with the well-known degeneracy of density profile versus velocity anisotropy. In this case acceptable fits can be obtained for all considered profiles, but only the profiles with cores yield good fits with anisotropy parameter close to the most natural isotropic value.

The amount of dark matter inferred depends on the concentration parameter of the density profile, but for realistic concentrations is typically of the order of $10^9 M_\odot$ both for Fornax and Draco for all profiles and velocity distributions. Since the total luminosity of Draco is two orders of magnitude lower than that of Fornax (see Table 1), this re-

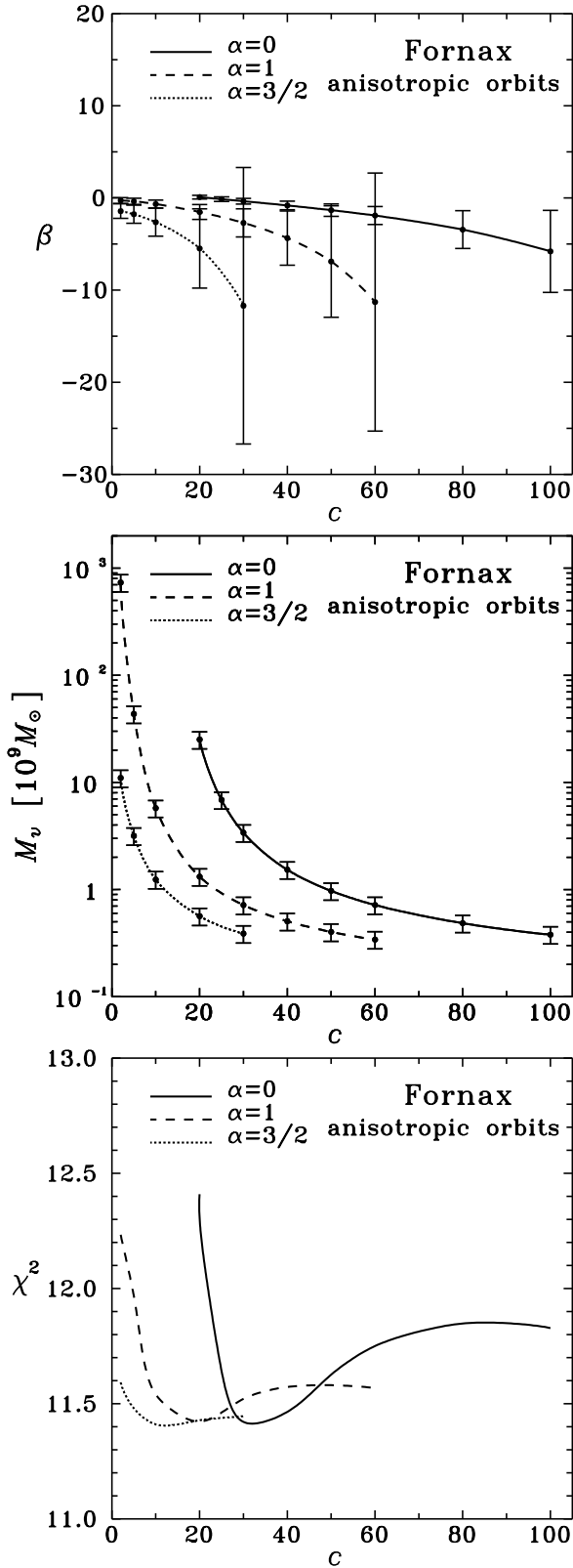


Figure 5. The best fitting anisotropy parameters β (upper panel) and masses of dark haloes (middle panel) as a function of assumed concentration parameter for profiles with different α in the case of anisotropic orbits for the Fornax dwarf. Lower panel: the goodness of fit measure, χ^2 , for the fits in the upper panels.

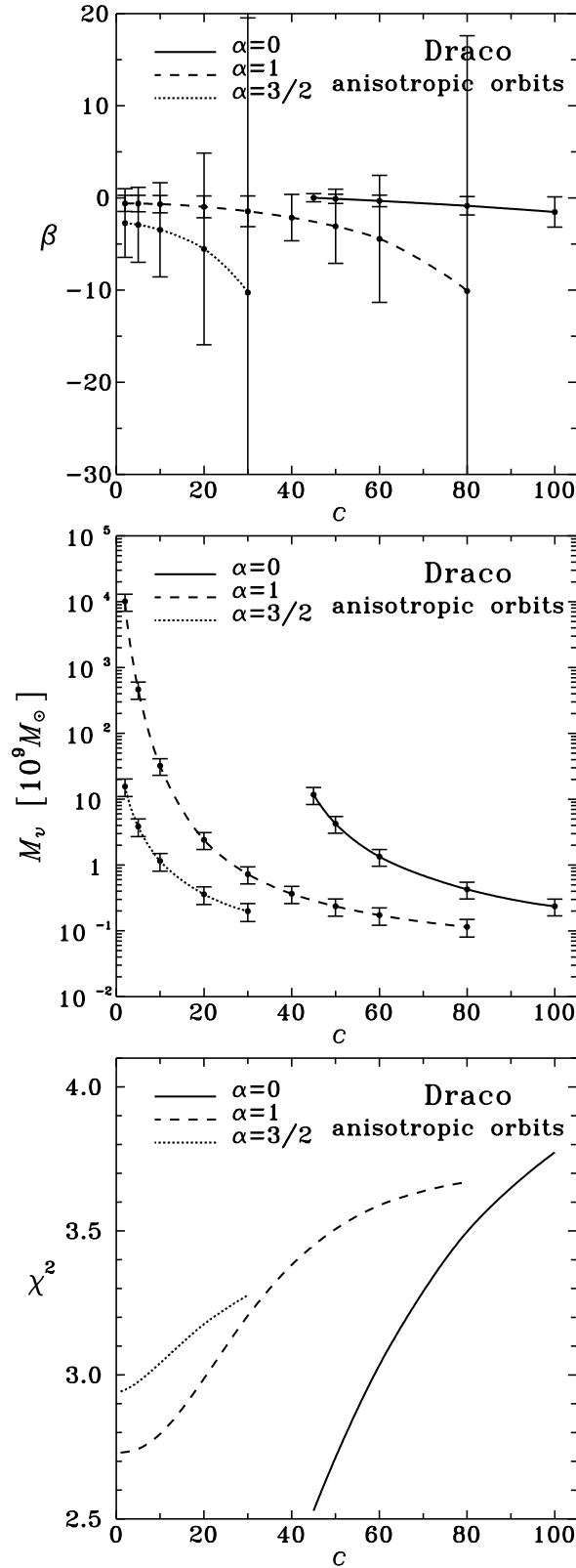


Figure 6. Same as Figure 5, but for Draco.

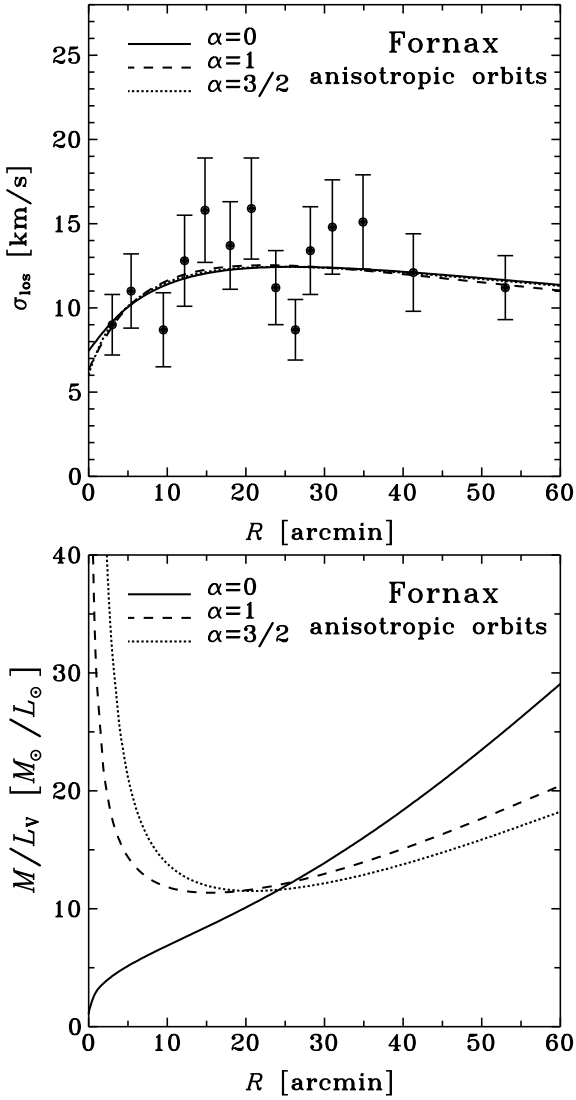


Figure 7. Upper panel: the best fitting velocity dispersion profiles obtained for $c = 30$ ($\alpha = 0$), $c = 20$ ($\alpha = 1$) and $c = 10$ ($\alpha = 3/2$) in the case of anisotropic orbits for the Fornax dwarf. Lower panel: mass-to-light ratios for the fits in the upper panel.

sults in a significant difference in their corresponding mass-to-light ratios. At the scale of the order of two Sérsic radii Fornax has $M/L_v \approx 10 M_\odot/L_\odot$ while for Draco we obtain $M/L_v \approx 100 M_\odot/L_\odot$. However, mass-to-light ratio dependence on distance is very different for different profiles. For cuspy profiles M/L_v diverges both at small and at large distances from the centre, while for $\alpha = 0$ profile it is finite at the centre and grows steadily with distance.

The results support the evidence based on studies of rotation curves of spiral galaxies which also favours density profiles with cores over those with cusps.

5.2 Alternative: MOND

DSph galaxies have low densities and therefore they lie in the regime of small accelerations. According to Modified

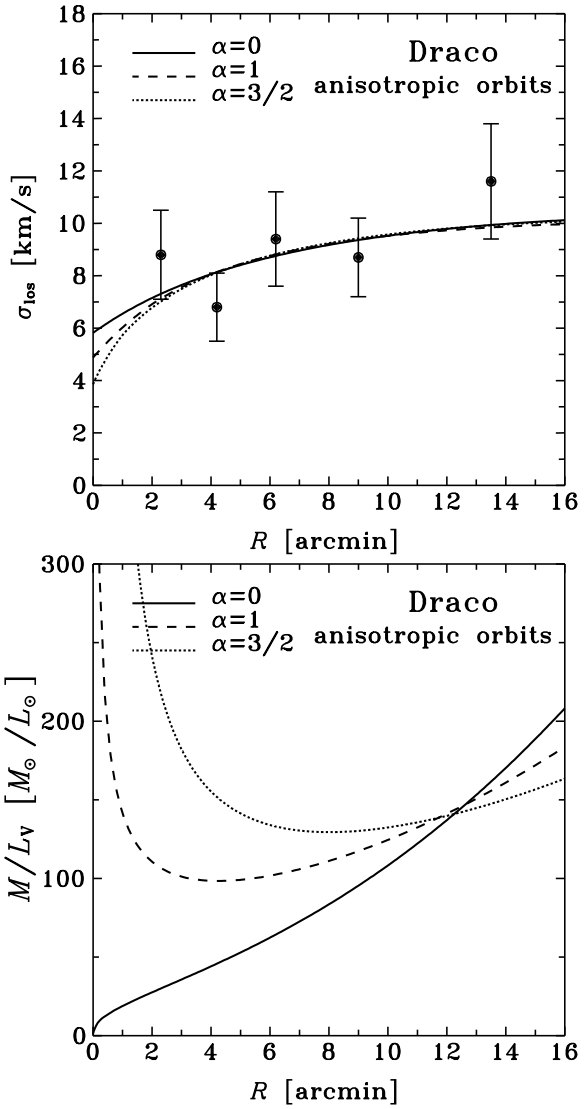


Figure 8. Same as Figure 7, but for Draco. The best fitting velocity dispersion profiles plotted were obtained for $c = 50$ ($\alpha = 0$), $c = 20$ ($\alpha = 1$) and $c = 10$ ($\alpha = 3/2$).

Newtonian Dynamics (MOND), the theory proposed by Milgrom (1983), for accelerations below the characteristic scale of $a_0 \approx 10^{-8} \text{ cm/s}^2$ the laws of Newtonian dynamics may change affecting either inertia or gravity and mimic the presence of dark matter. Although originally designed to explain flat rotation curves of spiral galaxies, MOND is expected to operate in all low-acceleration systems (it has been shown to explain e.g. many observed features of LSB galaxies by McGaugh & de Blok 1998) and in the case of dSph galaxies should cause an increase of velocity dispersions.

It is presently far from clear, whether MOND can explain the observed velocity dispersions of dSph galaxies. Although for most dwarfs it gives satisfactory results, notorious problems have been caused by Draco. Analyzing its central velocity dispersion Gerhard & Spergel (1992) have found it incompatible with stellar mass-to-light ratios, contrary to the conclusion of Milgrom (1995) who claimed that

its mass-to-light ratio is consistent with stellar values if all the observational errors are properly taken into account.

In the previous work (Lokas 2001) we have shown how to generalize the method of predicting the line-of-sight velocity dispersion profile to MOND and applied it to fit the data for Fornax, Draco and Ursa Minor dwarfs. We have assumed the stellar mass-to-light ratio of $M/L_V = 1M_\odot/L_\odot$ and fitted parameters a_0 and β . The best-fitting values of a_0 were different for different dwarfs, acceptable for Fornax, but much higher than expected in the case of Draco and Ursa Minor. We concluded that while the case of Ursa is doubtful since it has been recently observed to possess tidal tails (Martínez-Delgado et al. 2001), the high value of a_0 estimated for Draco can pose a serious problem for MOND (a similar conclusion based on the analysis of a velocity dispersion profile of Draco based on a different data set was also recently reached by Kleyna et al. 2001b).

We have repeated the analysis here for Fornax and Draco with the least-square fitting method, similar to that applied to fit dark matter profiles, in order to provide the error estimates for the fitted parameters. Both isotropic and anisotropic cases were studied. The results of the fitting procedure are shown in Table 3 with the isotropic case in the upper part and the anisotropic in the lower. We assumed $M/L_V = 1M_\odot/L_\odot$ and fitted the acceleration parameter a_0 in one case while taking $a_0 = 1.2 \times 10^{-8} \text{ cm/s}^2$, the value known to fit best the rotation curves of spiral galaxies (Begeaman, Broeils & Sanders 1991; Sanders & Verheijen 1998), and finding M/L_V in the other.

As is clear from Table 3 both approaches yield acceptable values of M/L_V or a_0 in the case of Fornax, while very high numbers in the case of Draco. However, the errors for Draco estimated from the uncertainties in the velocity dispersion measurements are so large that the acceptable values of M/L_V or a_0 (of the order of unity in the units of the Table) are still within 3σ error bars. Analysis of the velocity dispersion profile therefore reduces the error significantly compared to what can be obtained from a single central velocity dispersion measurement (then acceptable M/L_V are within 2σ error from the best-fitting value, McGaugh, private communication), but still not enough to rule out MOND. In fact these errors are farther increased if the error in luminosity measurement (quite big in the case of Draco, see Table 1) is taken into account. The resulting larger errors are given in brackets in Table 3. With these errors the values obtained here are safely within 2σ of the acceptable ones. (This source of error is not important for dark matter because it dominates strongly the distribution of stars.) We therefore conclude that with present quality of the data the alternative explanation of velocity dispersions in terms of MOND cannot yet be ruled out.

5.3 Alternative: tidal interactions

The analysis presented in this paper is valid under the condition that dSph galaxies are in dynamical equilibrium. However, those of them studied here, as members of the Local Group exist in gravitational field of larger galaxy, the Milky Way. One may worry that the tidal interactions with bigger galaxy may affect the dynamics of some dwarfs and our interpretations of their velocity dispersions. Some of the dwarfs have been indeed observed to possess tidal tails,

Table 3. Best-fitting parameters for MOND in the isotropic and anisotropic case with 1σ error bars. a_0 is given in units of 10^{-8} cm/s^2 , while M/L_V in M_\odot/L_\odot .

case	assumed	fitted	Fornax	Draco
$\beta = 0$	$M/L_V = 1$	a_0	$2.2 \pm 0.5(0.8)$	$39 \pm 13(22)$
	$a_0 = 1.2$	M/L_V	$1.8 \pm 0.4(0.7)$	$32 \pm 10(18)$
$\beta \neq 0$	$M/L_V = 1$	a_0	$2.1 \pm 0.5(0.8)$	$50 \pm 19(29)$
		β	-0.96 ± 0.53	-1.5 ± 1.6
	$a_0 = 1.2$	M/L_V	$1.8 \pm 0.4(0.7)$	$40 \pm 14(23)$
		β	-0.97 ± 0.53	-1.5 ± 1.7

e.g. Ursa Minor (Martínez-Delgado et al. 2001), Sagittarius (Ibata, Gilmore & Irwin 1994) or Carina (Majewski et al. 2000). It is still debated, whether this effect is common among dSph galaxies and whether it may cause an increase of velocity dispersion that is likely to be interpreted as presence of dark matter.

Tidal interactions have been studied theoretically by numerical modelling. Piatek & Pryor (1995) have performed numerical simulations of such effects and concluded that they should not affect much the inferred mass-to-light ratios. However, Kroupa (1997) and Klessen & Kroupa (1998) have demonstrated that what appears to be a dSph galaxy in equilibrium may in fact be a tidal remnant displaying high velocity dispersions without any dark matter. As suggested by Oh, Lin & Aarseth (1995) it may also very well be that some dwarfs indeed contain dark matter while others may be part of tidal debris.

ACKNOWLEDGEMENTS

I am grateful to Y. P. Jing for providing the results for the concentration of dark matter haloes in numerical form. I also wish to thank P. Salucci for encouragement to follow the line of investigation presented in this paper and S. McGaugh for discussions on dSph galaxies in MOND. This research was partially supported by the Polish State Committee for Scientific Research grant No. 2P03D02319.

REFERENCES

Armandroff T. E., Olszewski E. W., Pryor C., 1995, AJ, 110, 2131
 Armandroff T. E., Pryor C., Olszewski E. W., 1997, in Sofue Y., ed., Proc. IAU Symp. 184, The Central Regions of the Galaxy and Galaxies. Kluwer, Dordrecht, p. 35
 Avila-Reese V., Firmani C., Hernandez X., 1998, ApJ, 505, 37
 Begeman K. G., Broeils A. H., Sanders R. H., 1991, MNRAS, 249, 523
 Binney J., Mamon G. A., 1982, MNRAS, 200, 361
 Binney J., Tremaine S., 1987, Galactic Dynamics. Princeton Univ. Press, Princeton, chap. 4.
 Borriello A., Salucci P., 2001, MNRAS, 323, 285
 Burkert A., 1995, ApJ, 447, L25
 Caon N., Capaccioli M., D'Onofrio M., 1993, MNRAS, 265, 1013
 Caldwell N., 1999, AJ, 118, 1230
 Ciotti L., 1991, A&A, 249, 99
 de Blok W. J. G., McGaugh S. S., Bosma A., Rubin V. C., 2001, ApJ, 552, L23

de Blok W. J. G., McGaugh S. S., Rubin V. C., 2001, AJ, 122, 2396

El-Zant A., Shlosman I., Hoffman Y., 2001, ApJ, 560, 636

Flores R. A., Primack J. R., 1994, ApJ, 427, L1

Fukushige T., Makino J., 1997, ApJ, 477, L9

Gerhard O. E., Spergel D. N., 1992, ApJ, 397, 38

Gerhard O., Kronawitter A., Saglia R. P., Bender R., 2001, AJ, 121, 1936

Hannestad S., 1999, astro-ph/9912558

Hiotelis N., 2001, A&A, in press, astro-ph/0111324

Ibata R. A., Gilmore G. & Irwin M. J., 1994, Nature, 370, 194

Irwin M., Hatzidimitriou D., 1995, MNRAS, 277, 1354

Jing Y. P., Suto Y., 2000, ApJ, 529, L69

Kaplinghat M., Knox L., Turner M. S., 2000, Phys. Rev. Lett., 85, 3335

Klessen R. S., Kroupa P., 1998, ApJ, 498, 143

Kleyna J. T., Wilkinson M. I., Evans N. W., Gilmore G., 2001a, MNRAS, in press, astro-ph/0109450

Kleyna J. T., Wilkinson M. I., Evans N. W., Gilmore G., 2001b, ApJL, in press, astro-ph/0111329

Kroupa P., 1997, NewA, 2, 139

Lacey C., Cole S., 1993, MNRAS, 262, 627

Lima Neto G. B., Gerbal D., Márquez I., 1999, MNRAS, 309, 481

Lokas E. L., 2000, MNRAS, 311, 423

Lokas E. L., 2001, MNRAS, 327, 21P

Lokas E. L., Hoffman Y., 2000, ApJ, 542, L139

Lokas E. L., Mamon G. A., 2001, MNRAS, 321, 155

Majewski S. R., Ostheimer J. C., Patterson R. J., Kunkel W. E., Johnston K. V., Geisler D., 2000, AJ, 119, 760

Martínez-Delgado D., Alonso-García J., Aparicio A., Gómez-Flechos M. A., 2001, ApJ, 549, L63

Mateo M., 1997, in Arnaboldi M. et al., eds, ASP Conf. Ser. Vol. 116, The Nature of Elliptical Galaxies. Astron. Soc. Pac., San Francisco, p. 259

Mateo M., 1998, in Richtler T., Braun J. M., eds, Proc. Bonn/Bochum-Graduiertenkolleg Workshop, The Magellanic Clouds and Other Dwarf Galaxies. Shaker Verlag, Aachen, p. 53

Mateo M., Olszewski E. W., Welch D. L., Fischer P., Kunkel W., 1991, AJ, 102, 914

McGaugh S. S., de Blok W. J. G., 1998, ApJ, 499, 66

Merritt D., 1985, AJ, 90, 1027

Milgrom M., 1983, ApJ, 270, 365

Milgrom M., 1995, ApJ, 455, 439

Moore B., Governato F., Quinn T., Stadel J., Lake G., 1998, ApJ, 499, L5

Navarro J. F., Frenk C. S., White S. D. M., 1997, ApJ, 490, 493

Oh K. S., Lin D. N. C., Aarseth S. J., 1995, ApJ, 442, 142

Osipkov L. P., 1979, PAZh, 5, 77

Piatek S., Pryor C., 1995, AJ, 109, 1071

Ravindranath S., Ho L. C., Filippenko A. V. 2001, ApJ, in press, astro-ph/0110441

Richstone D. O., Tremaine S., 1984, ApJ, 286, 27

Salucci P., Burkert A., 2000, ApJ, 537, L9

Sanders R. H., Verheijen M. A. W., 1998, ApJ, 503, 97

Sérsic J. L., 1968, Atlas de Galaxias Australes, Observatorio Astronomico, Cordoba

Thomas P. A. et al., 1998, MNRAS, 296, 1061

van der Marel R. P., Magorrian J., Carlberg R. G., Yee H. K. C., Ellingson E., 2000, AJ, 119, 2038

White S. D. M., Zaritsky D., 1992, ApJ, 394, 1

Wilkinson M. I., Kleyna J. T., Evans N. W., Gilmore G., 2001, MNRAS, in press, astro-ph/0109451